International Journal of Wildland Fire **2019, 28, 329–341**
doi:10.1071/IS17021_AC

Supplementary material

Abrupt regime shifts in post-fire resilience of Mediterranean mountain pinewoods are fuelled by land use

J. Julio Camarero[A,F], *Gabriel Sangüesa-Barreda*[A,B], *Sebastián Pérez-Díaz*[C], *Cristina Montiel Molina*[D], *Francisco Seijo*[E] *and José Antonio López-Sáez*[C]

[A]Instituto Pirenaico de Ecología (IPE-CSIC), Avda. Montañana 1005, E-50192 Zaragoza, Spain.
[B]Departamento de Ciencias Agroforestales, EiFAB, iuFOR-Universidad de Valladolid, Campus Duques de Soria, E-42004 Soria, Spain.
[C]Archaeobiology Group, Institute of History (CCHS-CSIC), Calle de Albasanz, 26, E-28037 Madrid, Spain.
[D]Department of Geography, Complutense University of Madrid, C/ Profesor Aranguren s/n, E-28040 Madrid, Spain.
[E]IE School of International Relations, Calle de María de Molina 13, E-28006 Madrid, Spain.
[F]Corresponding author. Email: jjcamarero@ipe.csic.es

Supplementary material S1. Paleoecological methods

The modern vegetation of the peat bog includes *Caricetum carpetanae* communities dominated by *Carex nigra*, *C. echinata* and *Parnassia palustris* (Sánchez-Mata 1989). The vegetation of the area combines Maritime pine forests (*Pinus pinaster*), and *Pinus nigra* subsp. *salzmannii* woodlands with *Genista cinerascens* and *Festuca elegans* subsp. *merinoi* (López-Sáez *et al.* 2016). Overall, the high-supramediterranean belt has the lowest vegetation cover, with a predominance of grasslands, *Juniperus communis* subsp. *alpina* and broom communities (*Cytisus oromediterraneus*, *Echinospartum ibericum*), as well as scattered *Pinus sylvestris* and *P. nigra* subsp. *salzmannii* stands.

A 50-cm sediment core was extracted from "Arroyo de Aguas Frías" peat bog in October 2000 using a Russian corer with a diameter of 50 mm. Peat sections were individually sealed and stored at 4°C prior to laboratory sub-sampling at 1 cm intervals. Five peat samples were ^{14}C dated using AMS technique (Table S1). The AMS dating was conducted at the Centro Nacional de Aceleradores (CNA) Laboratory (Sevilla, Spain). Radiocarbon dates were calibrated in years cal AD with the CALIB 7.10 software using the calibration curve IntCal13 (Reimer *et al.* 2013). Dates are expressed as intercepts with 2σ ranges. An age-depth model (Fig. S1) was produced using Clam 2.2 software (Blaauw 2010). The best fit was obtained applying a smoothing spline to the available radiocarbon dates. Pollen analysis was carried out on 50 sub-samples of 1 cm^3 along the core length. Standard pollen extraction techniques were employed (Faegri and Iversen 1989). Pollen counts of up to 400 grains total land pollen (TLP) per sample were identified and counted. Percentages were calculated based on TLP sum excluding wetland taxa and non-pollen palynomorphs (NPPs). Pollen diagrams based on these data were produced using Tilia and Tilia-Graph v. 2.0.b.5 software (Grimm 1992, 2004). Pollen grains, spores and NPPs were identified using palynological keys and photo atlases (Moore *et al*. 1991; Reille 1999; Cugny *et al*. 2010). Additionally, *Pinus pinaster* was identified according to Carrión et al. (2000). Local pollen assemblage zones (LPAZs) were defined on the basis of agglomerative cluster analysis of incremental sum of squares (Coniss) with square root transformed percentage data (Grimm 1987). The number of statistically significant zones was determined using the broken-stick model (Bennett 1996).

Contiguous 1 cm^3 sub-samples were retrieved at 1 cm intervals for macroscopic charcoal analysis. Samples were soaked in a 10% NaOH solution for 24 h to disaggregate organic silts, then in a 6% H_2O_2 solution (24 h) to bleach the remaining non-charcoal organic material and thus make charcoal identification easier (Carcaillet et al., 2001). Samples were

gently wet sieved through a 150 µm mesh. The total number of macrocharcoal particles was counted using a stereomicroscope in order to estimate past changes in fire activity at a local scale (Whitlock and Larsen 2001, Higuera *et al*. 2007, Brown *et al*. 2013). Charcoal accumulation rate (CHAR) was calculated by sedimentation rate (cm $year^{-1}$) and is expressed in particles cm^{-2} $year^{-1}$ (Long and Whitlock 2002).

Table S1. Accelerator Mass Spectrometry radiocarbon (AMS-^{14}C) data with 2σ range of calibration from "Arroyo de Aguas Frías" peat bog.

Laboratory code	Depth (cm)	AMS ^{14}C age BP (yrs.)	Age cal AD	Mean Age cal AD
CNA-111	50	230 ± 30	1532-1950	1737
CNA-112	37	143 ± 20	1669-1944	1802
CNA-113	33	75 ± 30	1691-1923	1847
CNA-114	25	67 ± 20	1696-1919	1868
CNA-115	19	10 ± 30	1690-1960	1900

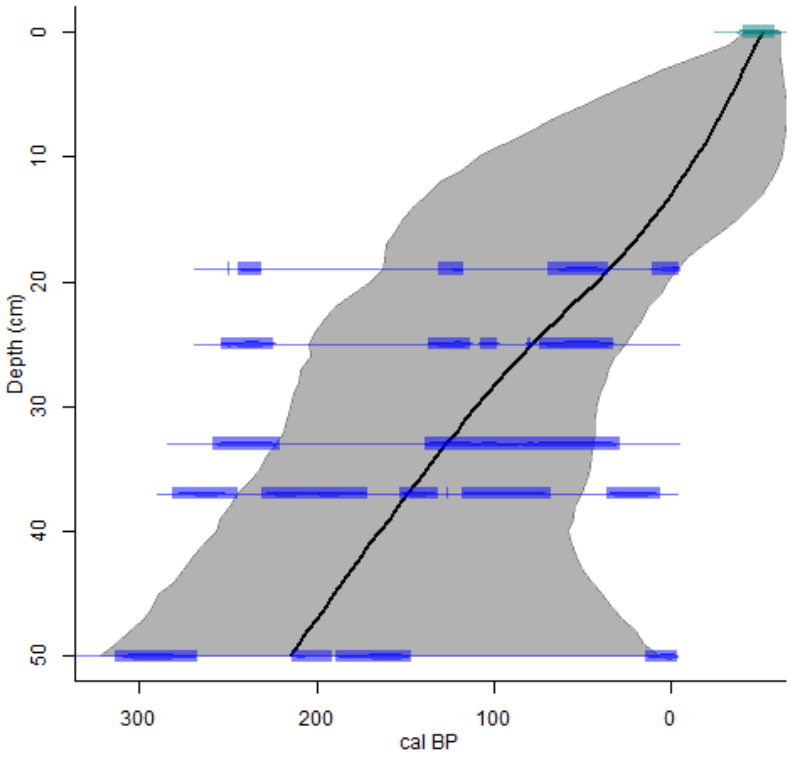

Fig. S1. Age-depth model from "Arroyo de Aguas Frías" peat bog.

References

Bennett KD (1996) Determination of the number of zones in a biostratigraphical sequence. *New Phytologist* **132**, 155–170.

Blaauw M (2010) Methods and code for "classical" age-modelling of radiocarbon sequences. *Quaternary Geochronology* **5**, 512–518.

Brown KJ, Power MJ (2013) 'Charred Particle Analysis'. Encyclopedia of Quaternary Science, pp. 716–729 (Elsevier: Amsterdam).

Carcaillet C, Bouvier M, Frechette B, Larouche AC, Richard PJH (2001) Comparison of pollen slide and sieving methods in lacustrine charcoal analyses for local and regional fire history. *The Holocene* **11**, 467–476.

Carrión JS, Navarro C, Navarro J, Munuera M (2000) The distribution of cluster pine (*Pinus pinaster*) in Spain as derived from palaeoecological data, relationships with phytosociological classification. *The Holocene* **10**, 243–252.

Cugny C, Mazier F, Galop D (2010) Modern and fossil non-pollen palynomorphs from the Basque mountains (western Pyrenees, France): the use of coprophilous fungi to reconstruct pastoral activity. *Vegetation History and Archaeobotany* **19**, 391–408.

Faegri K, Iversen J (1989) 'Textbook of pollen analysis.' (John Wiley: Chichester)

Grimm EC (1987) Coniss: a Fortran 77 program for stratigraphically constrained cluster analysis by the method of incremental sum of squares. *Computer and Geosciences* **13**, 13–35.

Grimm EC (1992) 'Tilia, version 2.'(Illinois State Museum: Springfield)

Grimm EC (2004) 'TGView' (Illinois State Museum: Springfield)

Higuera PE, Peters ME, Brubaker LB, Gavin DG (2007) Understanding the origin and analysis of sediment-charcoal records with a simulation model. *Quaternary Science Reviews* **26**, 1790–1809.

Long CJ, Whitlock C (2002) Fire and vegetation history from the coastal rain forest of the Western Oregon Coast Range. *Quaternaty Research* **58**, 215–225.

López-Sáez JA, Sánchez-Mata D, Gavilán RG (2016) Syntaxonomical update on the relict groves of Scots pine (*Pinus sylvestris* L. var. *iberica* Svoboda) and Spanish black pine (*Pinus nigra* Arnold subsp. *salzmannii* (Dunal) Franco) in the Gredos range (central Spain). *Lazaroa* **37**, 153–172.

Moore PD, Webb JA, Collinson ME (Eds) (1991) 'Pollen analysis.' (Blackwell: Oxford)

Reille M (1999) ‘Pollen and spores from Europe and North Africa.’ (Laboratoire de Botanique Historique et Palynologie: Marseille)

Reimer PJ, Bard E, Bayliss A, Beck JW, Blackwell PG, Bronk Ramsey C, Buck CE, Cheng H, Edwards RL, Friedrich M, Grootes PM, Guilderson TP, Haflidason H, Hajdas I, Hatté C, Heaton TJ, Hoffmann DL, Hogg AG, Hughen KA, Kaiser KF, Kromer B, Manning SW, Niu M, Reimer RW, Richards DA, Scott EM, Southon JR, Staff RA, Turney CSM, Van der Plicht J (2013) Intcal13 and marine13 radiocarbon age calibration curves 0–50,000 years cal BP. *Radiocarbon* **55**, 1869–1887.

Sánchez-Mata D (1989) ‘Flora y vegetación del Macizo Oriental de la Sierra de Gredos (Ávila).’ (Institución Gran Duque de Alba: Ávila).

Whitlock C, Larsen C (2001) Charcoal as a fire proxy. In Smol JP, Birks HJB, Last WM. (Eds.) ‘Tracking environmental change using lake sediments, vol. 3: terrestrial, algal, and siliceous indicators’, pp. 75–96 (Kluwer: Dordrecht).

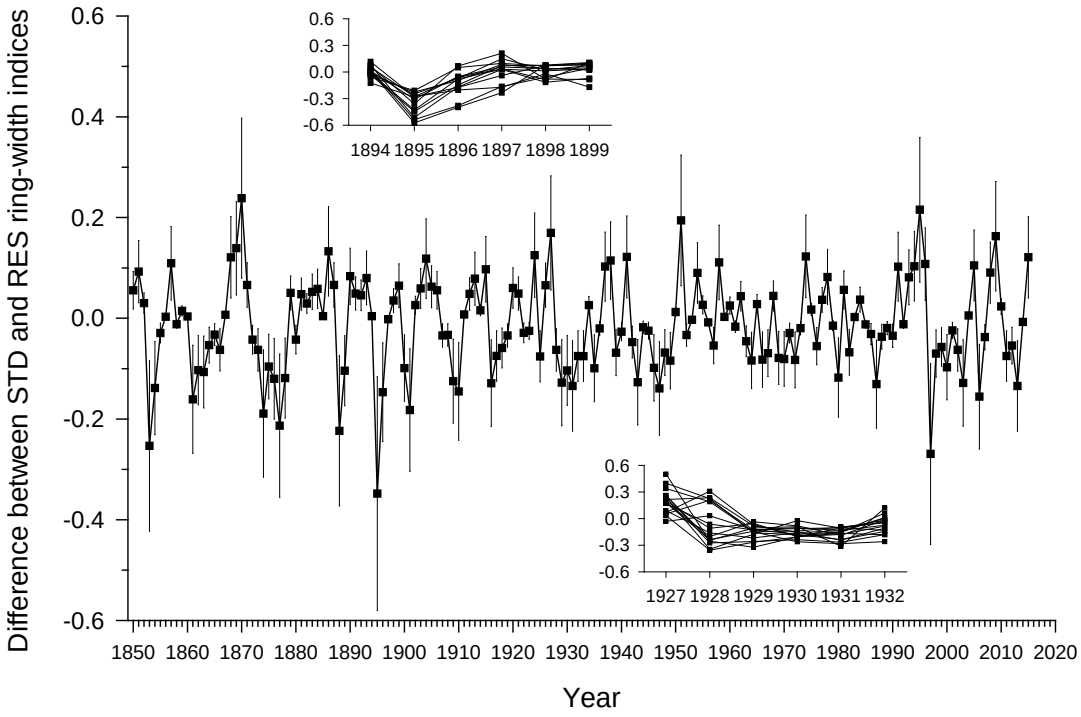

Fig. S2. Differences between the standard and residual ring-width indices observed in site TO (values are means ± standard errors) and details for two selected periods (insets) when historical fire frequency increased: 1894-1899 and 1927-1932.

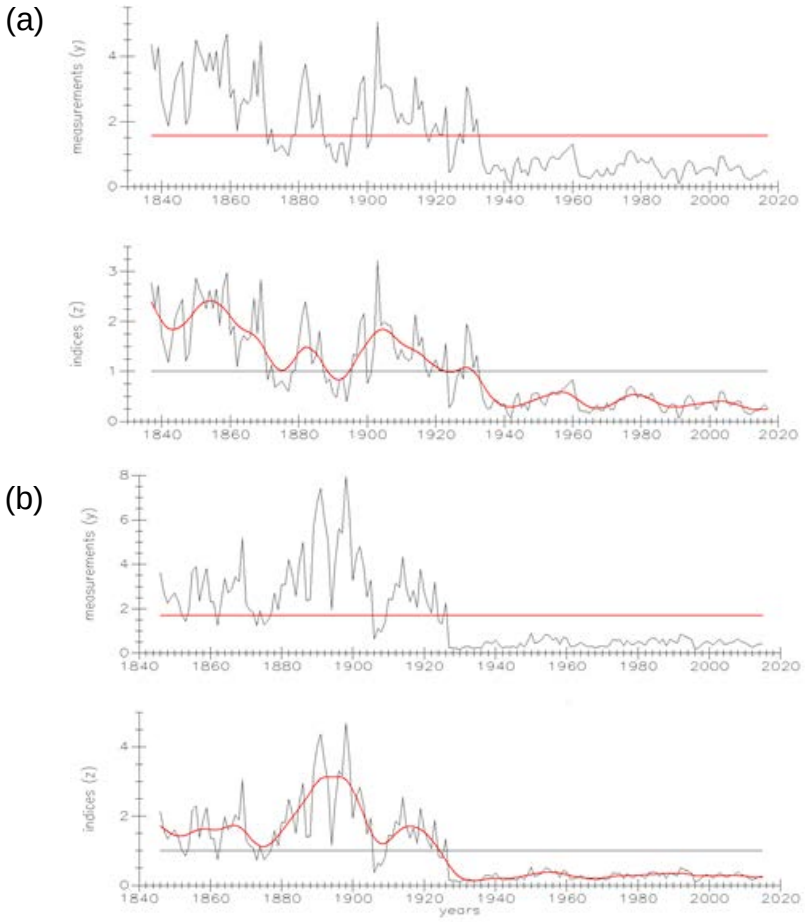

Fig. S3. Examples of trees sampled at sites CE (a) and TO (b) showing punctual and long-term growth declines in the 1890s and late 1920s, respectively. In each plot, the upper series show tree-ring width data (measurements in mm) and a fitted horizontal line, and the lower series show ring-width indices with a polynomial (spline) function.

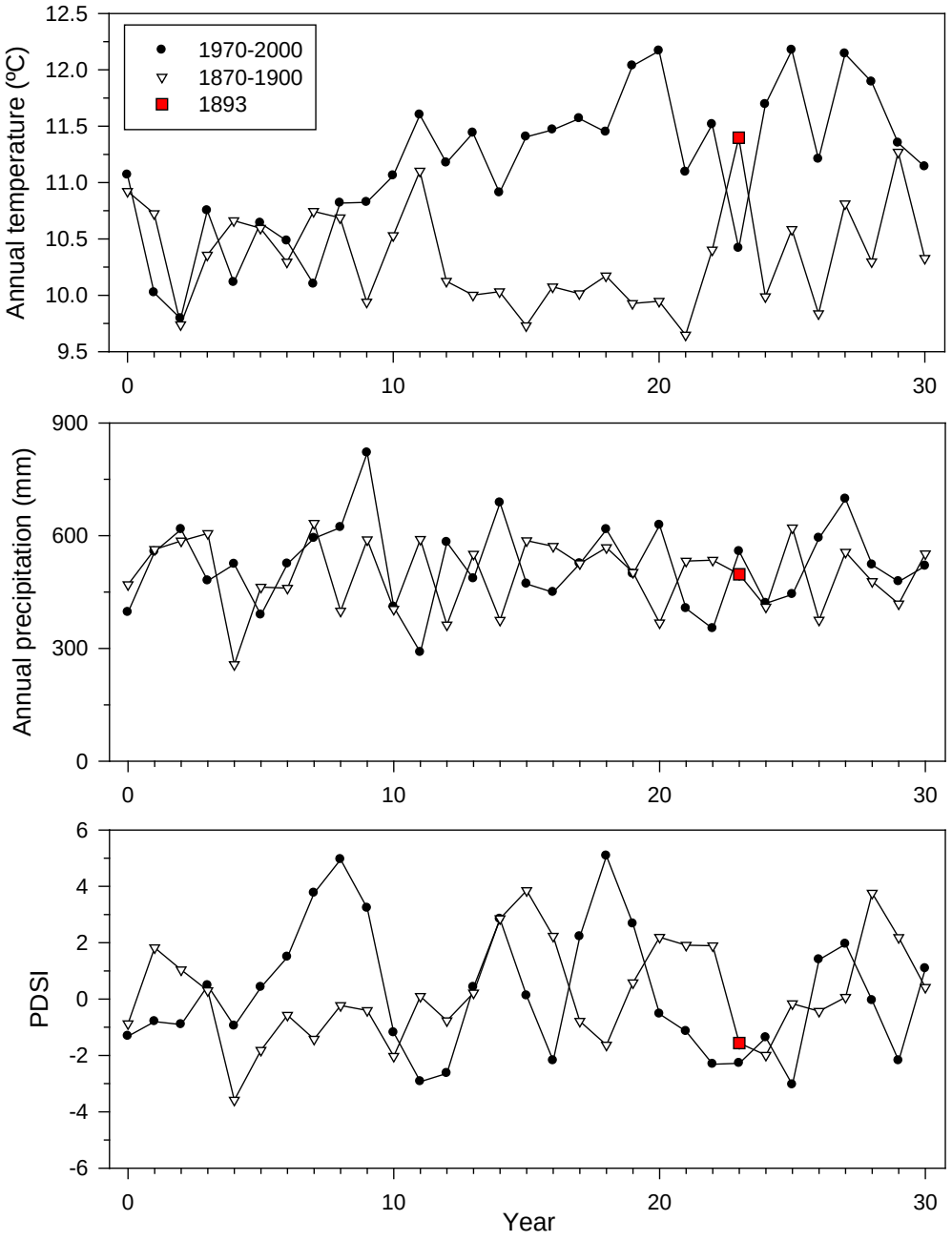

Fig. S4. Reconstructions of annual climate variables for the study area (means or total for the two 0.5º grids with coordinates 4.5º-5.0º W, 40.0º-40.5º N and 5.0º-5.5º W, 40.0-40.5º N) considering the last 31 years of the 19th (1870-1900) and 20th centuries (1970-2000). The square corresponds to 1893 when a high fire activity was observed according to historical records and paleoecological proxies (high charcoal accumulation rates, narrow tree rings). Temperature and precipitation reconstructions were produced by Luterbacher et al. (2004) and Pauling et al. (2006), respectively. The Palmer Drought Severity Index (PDSI) was obtained from the Old World Drought Atlas (Cook et al., 2015).

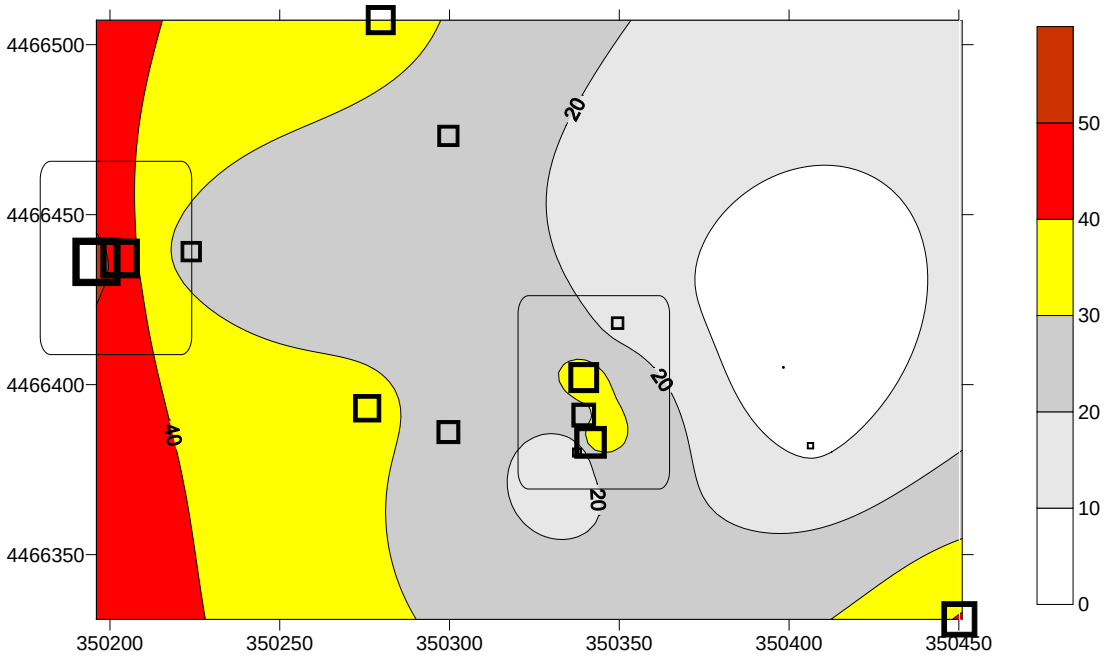

Fig. S5. Growth reduction is spatially associated to locations with fire-scarred trees. The plot shows tree sampled at site CE and the relative growth reduction (contour plot, color scale) expressed as negative growth changes (%). The symbols are trees and their size is proportional to the growth reduction. The two boxes highlight locations where all trees presented conspicuous fire scars (“catfaces”). The axes x (longitude) and y (latitude) correspond to UTM coordinates.

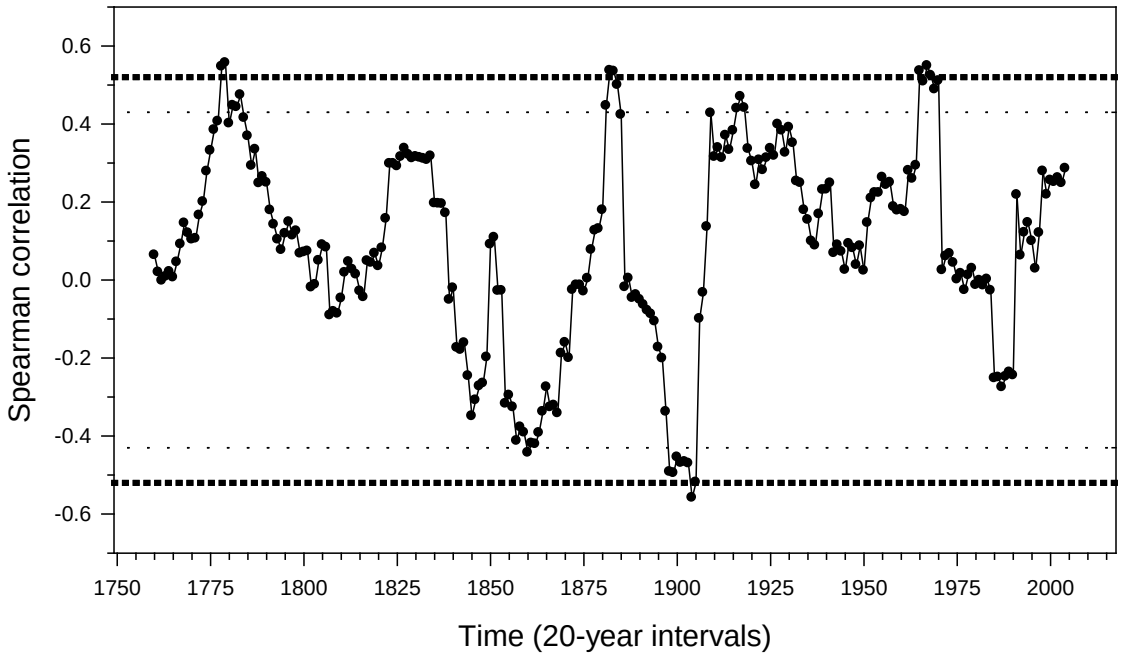

Fig. S6. Spearman moving correlations calculated by relating the annual number of fires according to historical records (Fig. 3a) and short-term changes in growth (differences between standard and residual ring-width indices, see Fig. 4a). Dashed and dotted horizontal lines show the 0.05 and 0.01 significance levels, respectively. Correlations were calculated for 20-year long intervals lagged by one year considering the common 1750-2013 period.